1-1-2003

First Measurement of Transferred Polarization in the Exclusive $\vec{e}$ p→e'K+$\vec{\Lambda}$ Reaction

D. S. Carman

Angela Biselli
Fairfield University, abiselli@fairfield.edu

CLAS Collaboration

Peer Reviewed

First Measurement of Transferred Polarization in the Exclusive $\vec{e}p \to e'K^+\vec{\Lambda}$ Reaction

D. S. Carman,[1] K. Joo,[2,3] M. D. Mestayer,[2] B. A. Raue,[4,2] G. Adams,[31] P. Ambrozewicz,[4] E. Anciant,[6] M. Anghinolfi,[19] D. S. Armstrong,[37] B. Asavapibhop,[25] G. Audit,[6] T. Auger,[6] H. Avakian,[18] H. Bagdasaryan,[38] J. P. Ball,[5] S. P. Barrow,[14] M. Battaglieri,[19] K. Beard,[22] M. Bektasoglu,[29,1] M. Bellis,[31] C. Bennhold,[15] N. Bianchi,[18] A. S. Biselli,[31] S. Boiarinov,[21] B. E. Bonner,[32] S. Bouchigny,[20,2] R. Bradford,[8] D. Branford,[13] W. J. Briscoe,[15] W. K. Brooks,[2] V. D. Burkert,[2] C. Butuceanu,[37] J. R. Calarco,[27] B. Carnahan,[9] A. Cazes,[34] C. Cetina,[15] L. Ciciani,[29] R. Clark,[8] P. L. Cole,[35,2] A. Coleman,[37] D. Cords,[2] P. Corvisiero,[19] D. Crabb,[3] H. Crannell,[9] J. P. Cummings,[31] E. DeSanctis,[18] P. V. Degtyarenko,[2] H. Denizli,[30] L. Dennis,[14] R. DeVita,[19] K. V. Dharmawardane,[29] K. S. Dhuga,[15] C. Djalali,[34] G. E. Dodge,[29] D. Doughty,[10,2] P. Dragovitsch,[14] M. Dugger,[5] S. Dytman,[30] O. P. Dzyubak,[34] M. Eckhause,[37] H. Egiyan,[37] K. S. Egiyan,[38] L. Elouadrhiri,[10,2] A. Empl,[31] P. Eugenio,[14] R. Fatemi,[3] G. Fedotov,[26] R. J. Feuerbach,[8] J. Ficenec,[36] T. A. Forest,[29] H. Funsten,[37] S. J. Gaff,[12] M. Gai,[11] M. Garçon,[6] G. Gavalian,[27,38] S. Gilad,[24] G. P. Gilfoyle,[33] K. L. Giovanetti,[22] P. Girard,[34] E. Golovach,[26] C. I. O. Gordon,[16] K. Griffioen,[37] S. Grimes,[1] M. Guidal,[20] M. Guillo,[34] L. Guo,[2] V. Gyurjyan,[2] C. Hadjidakis,[20] R. S. Hakobyan,[9] J. Hardie,[10,2] D. Heddle,[2,10] P. Heimberg,[15] F. W. Hersman,[27] K. Hicks,[1] R. S. Hicks,[25] M. Holtrop,[27] J. Hu,[31] C. E. Hyde-Wright,[29] B. Ishkhanov,[26] M. M. Ito,[2] D. Jenkins,[36] J. H. Kelley,[12] J. D. Kellie,[16] M. Khandaker,[28] K. Y. Kim,[30] K. Kim,[23] W. Kim,[23] A. Klein,[29] F. J. Klein,[9,2] A. V. Klimenko,[29] M. Klusman,[31] M. Kossov,[21] L. H. Kramer,[4,2] Y. Kuang,[37] S. E. Kuhn,[29] J. Kuhn,[31] J. Lachniet,[8] J. M. Laget,[6] D. Lawrence,[25] J. Li,[31] K. Livingston,[16] A. Longhi,[9] K. Lukashin,[2] J. J. Manak,[2] C. Marchand,[6] T. Mart,[17,15] S. McAleer,[14] J. McCarthy,[3] J. W. C. McNabb,[8] B. A. Mecking,[2] S. Mehrabyan,[30] J. J. Melone,[16] C. A. Meyer,[8] K. Mikhailov,[21] R. Minehart,[3] M. Mirazita,[18] R. Miskimen,[25] V. Mokeev,[26] L. Morand,[6] S. A. Morrow,[20] M. U. Mozer,[1] V. Muccifora,[18] J. Mueller,[30] L. Y. Murphy,[15] G. S. Mutchler,[32] J. Napolitano,[31] R. Nasseripour,[4] S. O. Nelson,[12] S. Niccolai,[15] G. Niculescu,[1] I. Niculescu,[15] B. B. Niczyporuk,[2] R. A. Niyazov,[29] M. Nozar,[2,28] G. V. O'Rielly,[15] A. K. Opper,[1] M. Osipenko,[26] K. Park,[23] K. Paschke,[8] E. Pasyuk,[5] G. Peterson,[25] N. Pivnyuk,[21] D. Pocanic,[3] O. Pogorelko,[21] E. Polli,[18] S. Pozdniakov,[21] B. M. Preedom,[34] J. W. Price,[7] Y. Prok,[3] D. Protopopescu,[27] L. M. Qin,[29] G. Riccardi,[14] G. Ricco,[19] M. Ripani,[19] B. G. Ritchie,[5] F. Ronchetti,[18] P. Rossi,[18] D. Rowntree,[24] P. Rubin,[33] F. Sabatié,[6,29] K. Sabourov,[12] C. Salgado,[28] J. Santoro,[36,2] V. Sapunenko,[19] R. A. Schumacher,[8] V. S. Serov,[21] Y. G. Sharabian,[2,38] J. Shaw,[25] S. Simionatto,[15] A. V. Skabelin,[24] E. S. Smith,[2] L. C. Smith,[3] D. I. Sober,[9] M. Spraker,[12] A. Stavinsky,[21] S. Stepanyan,[29,2] P. Stoler,[31] M. Taiuti,[19] S. Taylor,[32] D. J. Tedeschi,[34] U. Thoma,[2] R. Thompson,[30] L. Todor,[8] C. Tur,[34] M. Ungaro,[31] M. F. Vineyard,[33] A. V. Vlassov,[21] K. Wang,[3] L. B. Weinstein,[29] H. Weller,[12] D. P. Weygand,[2] C. S. Whisnant,[34] E. Wolin,[2] M. H. Wood,[34] A. Yegneswaran,[2] J. Yun,[29] B. Zhang,[24] J. Zhao,[24] and Z. Zhou[24]

(CLAS Collaboration)

[1]*Ohio University, Athens, Ohio 45701*
[2]*Thomas Jefferson National Accelerator Laboratory, Newport News, Virginia 23606*
[3]*University of Virginia, Charlottesville, Virginia 22901*
[4]*Florida International University, Miami, Florida 33199*
[5]*Arizona State University, Tempe, Arizona 85287*
[6]*CEA-Saclay, DAPNIA-SPhN, F91191 Gif-sur-Yvette Cedex, France*
[7]*University of California at Los Angeles, Los Angeles, California 90095*
[8]*Carnegie Mellon University, Pittsburgh, Pennsylvania 15213*
[9]*Catholic University of America, Washington, D.C. 20064*
[10]*Christopher Newport University, Newport News, Virginia 23606*
[11]*University of Connecticut, Storrs, Connecticut 06269*
[12]*Duke University, Durham, North Carolina 27708*
[13]*Edinburgh University, Edinburgh EH9 3JZ, United Kingdom*
[14]*Florida State University, Tallahassee, Florida 32306*
[15]*The George Washington University, Washington, D.C. 20052*
[16]*University of Glasgow, Glasgow G12 8QQ, United Kingdom*
[17]*Jurusan Fisika, FMIPA, Universitas Indonesia, Depok 16424, Indonesia*
[18]*INFN, Laboratori Nazionali di Frascati, P.O. 13,00044 Frascati, Italy*
[19]*INFN, Sezione di Genova and Dipartimento di Fisica, Università di Genova, 16146 Genova, Italy*
[20]*Institut de Physique Nucléaire d'ORSAY, IN2P3, BP1, 91406 Orsay, France*

[21]Institute of Theoretical and Experimental Physics, Moscow, 117259, Russia
[22]James Madison University, Harrisonburg, Virginia 22807
[23]Kyungpook National University, Taegu 702-701, South Korea
[24]Massachusetts Institute of Technology, Cambridge, Massachusetts 02139
[25]University of Massachusetts, Amherst, Massachusetts 01003
[26]Moscow State University, 119899 Moscow, Russia
[27]University of New Hampshire, Durham, New Hampshire 03824
[28]Norfolk State University, Norfolk, Virginia 23504
[29]Old Dominion University, Norfolk, Virginia 23529
[30]University of Pittsburgh, Pittsburgh, Pennsylvania 15260
[31]Rensselaer Polytechnic Institute, Troy, New York 12180
[32]Rice University, Houston, Texas 77005
[33]University of Richmond, Richmond, Virginia 23173
[34]University of South Carolina, Columbia, South Carolina 29208
[35]University of Texas at El Paso, El Paso, Texas 79968
[36]Virginia Polytechnic Institute and State University, Blacksburg, Virginia 24061
[37]College of William and Mary, Williamsburg, Virginia 23187
[38]Yerevan Physics Institute, 375036 Yerevan, Armenia

The first measurements of the transferred polarization for the exclusive $\vec{e}p \rightarrow e'K^+\vec{\Lambda}$ reaction have been performed at Jefferson Laboratory using the CLAS spectrometer. A 2.567 GeV beam was used to measure the hyperon polarization over Q^2 from 0.3 to 1.5 $(\text{GeV}/c)^2$, W from 1.6 to 2.15 GeV, and over the full K^+ center-of-mass angular range. Comparison with predictions of hadrodynamic models indicates strong sensitivity to the underlying resonance contributions. A nonrelativistic quark-model interpretation of our data suggests that the $s\bar{s}$ quark pair is produced with spins predominantly antialigned. Implications for the validity of the most widely used quark-pair creation operator are discussed.

We present here the first measurements of spin transfer in the nucleon resonance region from a longitudinally polarized-electron beam to the Λ hyperon produced in the exclusive $p(\vec{e}, e'K^+)\vec{\Lambda}$ reaction. Understanding nucleon resonance excitation continues to provide a major challenge to hadronic physics due to the nonperturbative nature of QCD at these energies. Studies of strange final states can potentially uncover baryonic resonances that do not couple or couple only weakly to the πN channel due to the different hadronic vertices. Recent symmetric quark models predict more states than have been found experimentally [1]. Whether these missing states do in fact exist is directly tied to the question of whether certain quark degrees of freedom might be "frozen out" as in, e.g., some diquark models [2]. This question is central to our understanding of baryon structure.

In the absence of direct QCD predictions, the theoretical framework involving hadrodynamic models has been extensively applied to the study of electromagnetic production of pseudoscalar mesons [3–6]. Their predictive powers, however, are still limited by a sparsity of data. Model fits to the existing cross section data are generally obtained at the expense of many free parameters, and these unpolarized data alone are not sufficiently sensitive to fully understand the reaction mechanism as they probe only a small portion of the full response. Our double-polarization data can provide significant new constraints on the basic parameters of these models, increasing their discriminatory power and allowing for a quantitative measure of whether or not new "missing" resonances might be required to explain these and other hyperon production data.

Alternatively, our data provide interesting, and perhaps surprising, information about the nature of quark-pair production. There is a growing body of evidence that the appropriate degrees of freedom to describe the phenomenology of hadronic decays are constituent quarks held together by a gluonic flux tube [7]. The nonperturbative nature of the flux tube gives rise to the well-known linear potential of heavy-quark confinement [8]. Other properties of the flux tube can be determined by studying $q\bar{q}$ pair production, since this is widely believed to produce the color field neutralization that actually breaks the flux tube.

Since the 1970s it has been suggested that a quark pair with vacuum quantum numbers is responsible for breaking the color flux tube (the $^3P_0$ model [9]). The most sensitive experiments to date have measured ratios in certain meson decays of strong amplitudes differing in their orbital angular momenta [10]. Since the $^3P_0$ operator has $S = 1$ and $L = 1$, it implies a different amplitude ratio than, e.g., a $^3S_1$ operator with $S = 1$ and $L = 0$, corresponding to one gluon exchange. Later, we will argue that the spin properties of the quark-pair creation operator might be responsible for the observed trends in the Λ polarization, which indicate that the relevant

operator dominating our reaction produces the $s\bar{s}$ pair with spins antialigned. This finding, if confirmed by further calculations, brings into question the universal applicability of the $^3P_0$ model. This has important implications since many, if not most, calculations of hadronic spectroscopy use the $^3P_0$ operator to calculate the transition to the final-state particles [11].

Jefferson Laboratory provides multi-GeV electron beams with longitudinal polarization up to 80%. The CLAS spectrometer [12] in Hall B of this facility is constructed around six superconducting coils that generate a toroidal magnetic field to momentum analyze charged particles. The detection system consists of drift chambers to determine charged-particle trajectories, Čerenkov detectors for electron/pion separation, scintillation counters for flight-time measurements, and calorimeters to identify electrons and high-energy neutral particles. Operating luminosity with the unpolarized liquid-H_2 target is $\sim 1 \times 10^{34}$ cm^{-2} s^{-1}.

The large acceptance of CLAS has enabled us to detect the final-state electron and kaon, and the proton from the decay of the Λ hyperon at a beam energy of 2.567 GeV, over a range of momentum transfer Q^2 from 0.3 to 1.5 (GeV/c)^2 and invariant energy W from 1.6 to 2.15 GeV, while providing full angular coverage in the kaon center of mass (c.m.). Hyperon identification with CLAS relies on missing-mass reconstructions. Figure 1(a) shows the missing mass for $p(e, e'K^+)X$ where a proton has also been detected. Figure 1(b) shows the missing mass for $p(e, e'K^+ p)X$, where the final-state proton can come from the decay of the $\Lambda(1115)$ (missing π^-) or the $\Sigma^0(1192)$ (missing $\pi^-\gamma$). Figure 1(c) shows the resulting hyperon spectrum after a cut on the π^- peak in Fig. 1(b).

An attractive feature of the $\Lambda \to p\pi^-$ decay comes from its self-analyzing nature. This weak decay has an asymmetric angular distribution with respect to the Λ spin direction such that the decay-proton distribution in the Λ rest frame (RF) for each beam helicity state (+ or $-$) is of the form:

$$\frac{dN^\pm}{d\cos\theta_p^{\mathrm{RF}}} = N[1 + \alpha(P^0 \pm P_b P')\cos\theta_p^{\mathrm{RF}}], \qquad (1)$$

where P_b is the average beam polarization and $\alpha = 0.642 \pm 0.013$ is the weak decay asymmetry parameter [13]. The Λ polarization is the sum of P^0, the induced polarization, and P', the helicity-dependent transferred polarization, both defined with respect to a particular set of spin-quantization axes. This latter quantity is the focus of this work. Figure 2 highlights two standard choices for the spin-quantization axes.

Using Eq. (1), we can express the acceptance-corrected yield asymmetries in terms of the average transferred polarization for each kinematic bin as

$$A_\xi(\cos\theta_p^{\mathrm{RF}}) = \frac{N_\xi^+ - N_\xi^-}{N_\xi^+ + N_\xi^-} = \frac{\alpha P_b \cos\theta_p^{\mathrm{RF}} P_\xi'}{1 + \alpha P_\xi^0 \cos\theta_p^{\mathrm{RF}}}. \qquad (2)$$

Here $N_\xi^\pm(\cos\theta_p^{\mathrm{RF}})$ are the decay-proton helicity-gated yields with respect to the different spin-quantization axes $\xi = \hat{i}, \hat{j}, \hat{k}$, where θ_p^{RF} is the RF polar angle between the proton momentum and the chosen spin axis. To first order, the acceptance corrections cancel in the asymmetry of Eq. (2), however they have been included, and in fact, represent the largest source of systematic uncertainty in the polarization measurement [14].

Using the notation of Ref. [15], the most general form for the virtual photoabsorption c.m. cross section for our reaction from an unpolarized target, allowing for both a polarized-electron beam and recoil hyperon is given by

$$\frac{d\sigma_v}{d\Omega_K^*} = \mathcal{K} \sum_{\beta=0,x',y',z'} [R_T^{\beta 0} + \epsilon_L R_L^{\beta 0} + c_+({}^c R_{LT}^{\beta 0}\cos\Phi + {}^s R_{LT}^{\beta 0}\sin\Phi) + \epsilon({}^c R_{TT}^{\beta 0}\cos2\Phi + {}^s R_{TT}^{\beta 0}\sin2\Phi)$$
$$+ hc_-({}^c R_{LT'}^{\beta 0}\cos\Phi + {}^s R_{LT'}^{\beta 0}\sin\Phi) + hc_0 R_{TT'}^{\beta 0}]. \qquad (3)$$

The $R_i^{\beta\alpha}$ are the transverse, longitudinal, and interference response functions that relate to the underlying hadronic current and implicitly contain the Λ polarization. The sum over β includes contributions from the polarization with respect to the (x', y', z') axes (see Fig. 2). The $\beta = 0$ terms account for the unpolarized response and $\alpha = 0$ implies an unpolarized target. Here $c_\pm = \sqrt{2\epsilon_L(1 \pm \epsilon)}$ and $c_0 = \sqrt{1 - \epsilon^2}$, where ϵ [$\epsilon_L = \epsilon Q^2/(k_\gamma^{\mathrm{c.m.}})^2$] is the transverse (longitudinal) polarization of the virtual photon, $\mathcal{K} = |\vec{q}_K|/k_\gamma^{\mathrm{c.m.}}$, $k_\gamma^{\mathrm{c.m.}}$ is the virtual photon c.m. momentum, h is the beam helicity, and Φ is the angle between the electron and hadron planes. The c and s labels indicate whether R_i multiplies a sine or cosine term.

Using Eq. (3), the polarization components in the (x', y', z') system are given by [16]

$$\sigma_0 P_\xi^0 = \mathcal{K}(c_+ {}^s R_{LT}^{\xi 0}\sin\Phi + \epsilon^s R_{TT}^{\xi 0}\sin2\Phi), \qquad \xi = x', z',$$

$$\sigma_0 P_{y'}^0 = \mathcal{K}(R_T^{y'0} + \epsilon_L R_L^{y'0} + c_+ {}^c R_{LT}^{y'0}\cos\Phi$$
$$+ \epsilon^c R_{TT}^{y'0}\cos2\Phi), \qquad (4)$$

$$\sigma_0 P_\xi' = \mathcal{K}(c_- {}^c R_{LT'}^{\xi 0}\cos\Phi + c_0 R_{TT'}^{\xi 0}), \qquad \xi = x', z',$$

$$\sigma_0 P_{y'}' = \mathcal{K}c_- {}^s R_{LT'}^{y'0}\sin\Phi. \qquad (5)$$

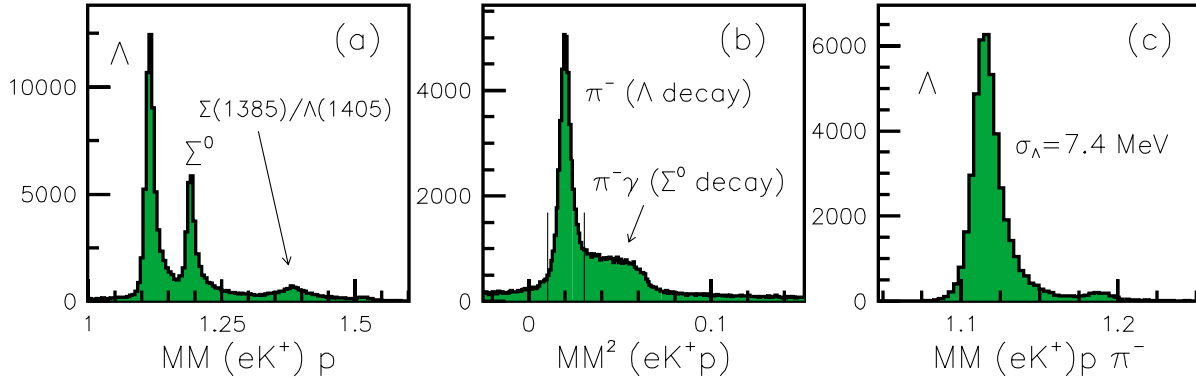Here σ_0 is the unpolarized cross section. These definitions

FIG. 1 (color online).   Missing-mass spectra (GeV) for the reactions (a) $p(e, e'K^+)X$ and (b) $p(e, e'K^+p)X$. (c) The hyperon distribution after cutting on the low-mass peak in (b). CLAS data from 2.567 GeV summing over all Q^2 and W.

can be related to the (x, y, z) system (see Fig. 2) via appropriate rotation operators.

The data were summed over all Φ angles to improve the statistical precision of the measurement. In the summation, the induced components $P^0_{x',z',x,z}$ and the transferred components $P'_{y',y}$ vanish identically. Thus the nonzero, helicity-gated yield asymmetries of Eq. (2) reduce to

$$A_\xi = \alpha P_b \cos\theta_p^{\mathrm{RF}} P'_\xi, \qquad \xi = \hat{i}, \hat{k}, \qquad (6)$$

allowing for a direct extraction of P' in a given kinematic bin with a linear fit of A_ξ to $\cos\theta_p^{\mathrm{RF}}$. Note that different choices for the spin axes lead to sensitivities of P' to different subsets of the response functions. The nonzero, Φ-integrated transferred polarization components in the (x', y', z') and (x, y, z) systems are given by

$$P'_{x'} = c_1 R^{x'0}_{TT'}, \qquad P'_{z'} = c_1 R^{z'0}_{TT'},$$
$$P'_x = c_2({}^cR^{x'0}_{LT'} \cos\theta^*_K - R^{y'0}_{LT'} + {}^sR^{z'0}_{LT'} \sin\theta^*_K), \qquad (7)$$
$$P'_z = c_1(-{}^sR^{x'0}_{TT'} \sin\theta^*_K + {}^cR^{z'0}_{TT'} \cos\theta^*_K).$$

The normalization factors are given by $c_1 = c_0/K_0$ and $c_2 = c_-/(2K_0)$, where $K_0 = R^{00}_T + \epsilon_L R^{00}_L$. This formalism is important to highlight as the hadrodynamic models provide the response functions in the (x', y', z') system as their outputs.

Our results are shown in Figs. 3 and 4 compared to several hadrodynamic model calculations. The error bars in these figures include statistical but not systematic uncertainties for P', which we estimate to be ≤ 0.084 on the polarization [14]. The dominant source of systematic effects comes from the acceptance correction (0.07). Other contributions include effects associated with binning, extraction methods, and the beam polarization uncertainty.

Figure 3 shows the W dependence of P' summed over all Q^2 and $d\Omega^*_K$ for our two choices of spin axes. The data indicate sizeable Λ polarizations. The average polarization magnitude is roughly the same along the z' and x' axes, indicating equal strength in the $R^{z'0}_{TT'}$ and $R^{x'0}_{TT'}$ responses. For the other choice of axes, the polarization is maximal when projected along the z axis (the virtual
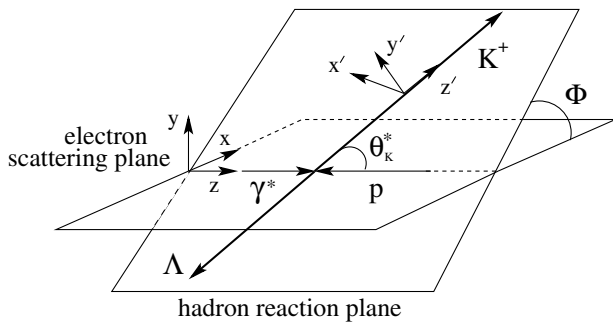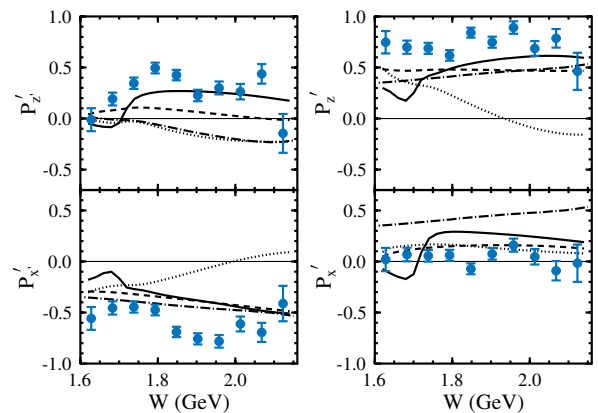

FIG. 2.   Center-of-mass coordinate system highlighting the definitions of the different spin-quantization axis choices for the final-state Λ hyperon used in the polarization analysis.

FIG. 3 (color online).   Transferred Λ polarization components $P'_{z'}$ and $P'_{x'}$ (left panel) and P'_z and P'_x (right panel) at 2.567 GeV vs W summed over all Q^2 and $d\Omega^*_K$. Curves correspond to the hadrodynamic models: WJC92 (dotted), BM98 (dashed), BM02 (solid), J02 (dot-dashed), averaged over the experimental bins.
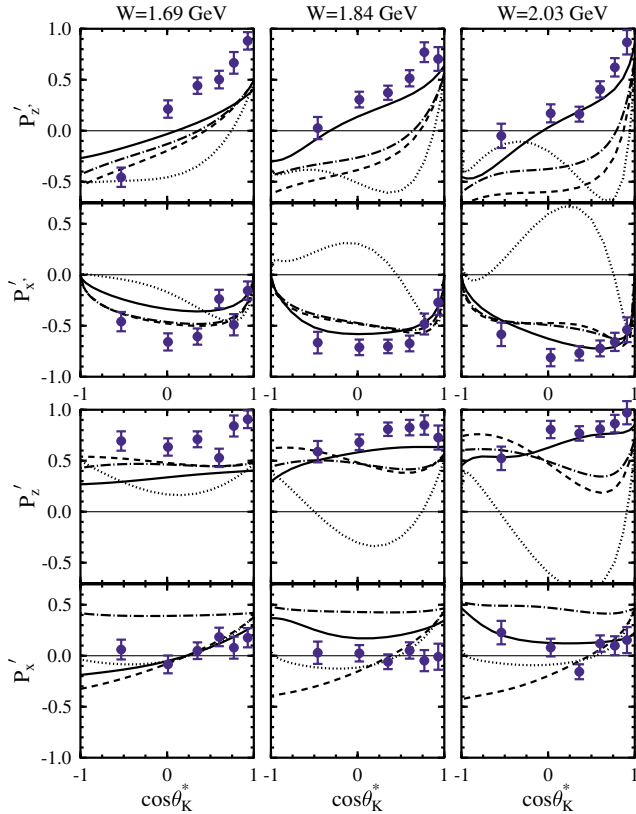
FIG. 4 (color online). Transferred Λ polarization components $P'_{z'}$ and $P'_{x'}$ (upper panels) and P'_z and P'_x (lower panels) at 2.567 GeV vs $\cos\theta^*_K$ summed over all Q^2 and Φ for three W bins centered at 1.69, 1.84, and 2.03 GeV. The curves are the same as in Fig. 3.

photon direction), while the component along the x axis is consistent with zero.

Figure 4 shows the angular dependence of P' summed over all Q^2 for three different W bins from just above threshold to 2 GeV. The polarization $P'_{z'}$ decreases with increasing θ^*_K. $P'_{x'}$ is constrained to be zero at $\cos\theta^*_K = \pm 1$ due to angular momentum conservation and reaches a minimum at $\theta^*_K \sim 90°$. Again, the maximum Λ polarization occurs along the virtual photon direction. This component, P'_z, is roughly constant with respect to $\cos\theta^*_K$ and W. The component P'_x in the electron-scattering plane is again consistent with zero. The Φ-integrated $P'_{y'}$ and P'_y components (not shown) are statistically consistent with zero with respect to W and $\cos\theta^*_K$ as expected [14].

Recent calculations have been guided by coupled-channels analyses [4,17] that recognize the importance of the $S_{11}(1650)$, $P_{11}(1710)$, and $P_{13}(1720)$ s-channel resonances, which are the only ones with a known significant branching into strange channels [13]. The $p(e, e'K^+)\Lambda$ cross section data exhibit a forward peaking in θ^*_K that has been attributed to t-channel exchanges [18]. For this reason the two lowest vector meson resonances

$K^*(892)$ and $K_1(1270)$ are typically included. Some models also include Y^* resonances in the u channel.

A comparison of the four models employed in this work is included in Table I. These models were developed by Williams, Ji, and Cotanch (WJC92) [3], Bennhold and Mart (BM02,BM98) [4,19], and Janssen (J02) [6]. They differ in their mix of N^* resonances, e.g., BM02 and J02 both include one of the missing quark-model states, the $D_{13}(1895)$. The most recent models (all but WJC92) have included form factors at the hadronic vertices. In this work, we have employed simple electromagnetic dipole form factors for the kaon and the hyperon. In general the calculations do not reproduce the data in Figs. 3 and 4, and while the comparison of the calculations to the data is illustrative to highlight the present deficiencies in the current models and their parameter values, the next step in the study of the reaction mechanism is to include our polarization data in the available database and to refit the set of coupling strengths.

As noted earlier, our data reveal a simple phenomenology that indicates the transferred Λ polarization is maximal along the virtual photon direction. Here, we have not included the virtual photon depolarization factor. For our data sample this factor is ~ 0.8, which if divided out, would push P' even closer to unity. We note that the lack of a strong W dependence is an indication that the data might be economically described in a flux-tube strong-decay framework. In this picture we expect that the cross section is dominated by photoabsorption by a u quark. When viewed in the γ^*-p Breit frame, after a u quark has absorbed the virtual photon, there is an intermediate u-(ud) system with the u quark polarized along the photon direction ($+z$) due to the helicity-conserving vector interaction. Hadronization into the K^+-Λ final state proceeds with the production of an $s\bar{s}$ pair that breaks the color flux tube. Because the u quark hadronizes as a pseudoscalar K^+, the $\bar{s}$ quark spin is required to be opposite to that of the u quark, i.e., in the $-z$ direction. In the nonrelativistic quark model the entire spin of the Λ is carried by the s quark. Since we observe the Λ polarization to be in the $+z$ direction, we conclude that the s and $\bar{s}$ spins were antialigned when they were created, if the hadronization did not flip or rotate their spins. We note that the authors of Ref. [20] also posit a two-step process

TABLE I. Resonances within the models highlighted in this work included with the nonresonant Born terms.

Resonance	WJC92	BM98	BM02	J02
$N^*(1650), N^*(1710)$	*	*	*	*
$N^*(1720), N^*(1895)$			*	*
$K^*(892)$	*	*	*	*
$K_1(1270)$	*		*	*
$\Lambda^*(1405)$	*			
$\Lambda^*(1800), \Lambda^*(1810)$				*

for the production of transversely polarized Λ hyperons in the exclusive $pp \to pK^+\Lambda$ reaction, and come to the similar conclusion that the s and $\bar{s}$ quark pair must also have been produced with spins antialigned.

A dominance of spin antialignment for the s and $\bar{s}$ quarks is not consistent with the $S = 1\,{}^3P_0$ operator, which predicts a 2:1 mixture of $s\bar{s}$ quarks produced with spins aligned versus antialigned if the orbital substates are equally populated. Along with other observations of failure of the ${}^3P_0$ model (e.g., explaining $\pi_2 \to \rho\omega$ decay [11]), the applicability of the ${}^3P_0$ model in describing all hadronic decays is brought into doubt. We await theoretical investigations on the effect of the functional form of the quark-pair-creation operator on hyperon polarizations when a single $s\bar{s}$ pair is produced.

We have reported the first double-polarization measurements in the resonance region for the $p(\vec{e}, e'K^+)\vec{\Lambda}$ reaction. Our data show a large degree of Λ polarization, which is maximal along the virtual photon direction (averaging $\sim 75\%$ for our kinematics). As this is the first polarization data set, inclusion into the available database should make hadrodynamic models much more reliable for studies of missing-resonance production. Additionally, we feel that a better handle on the form of the quark-pair creation operator will make baryon spectroscopic models more reliable, hence increasing our confidence in their predictions for missing resonances.

[1] S. Capstick and W. Roberts, Phys. Rev. D **58**, 074011 (1998).
[2] R. Alkofer *et al.*, Nucl. Phys. **A680**, 70 (2001).
[3] R. A. Williams *et al.*, Phys. Rev. C **46**, 1617 (1992).
[4] T. Mart and C. Bennhold, Phys. Rev. C **61**, 012201 (2000).
[5] B. Saghai, nucl-th/0105001.
[6] S. Janssen *et al.*, Phys. Rev. C **65**, 015201 (2002).
[7] N. Isgur and J. Paton, Phys. Rev. D **31**, 2910 (1985).
[8] G. S. Bali *et al.*, Phys. Rev. D **51**, 5165 (1995).
[9] A. LeYaouanc *et al.*, Phys. Rev. D **8**, 2223 (1973).
[10] P. Geiger and E. Swanson, Phys. Rev. D **50**, 6855 (1994).
[11] T. Barnes, hep-ph/0202157.
[12] B. A. Mecking *et al.*, Nucl. Instrum. Methods Phys. Res., Sect. A (to be published).
[13] D. E. Groom *et al.*, Eur. Phys. J. C **15**, 1 (2000).
[14] D. S. Carman and B. A. Raue, CLAS Analysis Note No. 02-018, 2002, see www.jlab.org/Hall-B/notes/.
[15] G. Knöchlein *et al.*, Z. Phys. A **352**, 327 (1995).
[16] H. Schmieden, Eur. Phys. J. A **1**, 427 (1998).
[17] T. Feuster and U. Mosel, Phys. Rev. C **59**, 460 (1999).
[18] K. H. Hicks, in *Proceedings of Hadron2001*, edited by D. Amelin and A. Zaitsev, AIP Conf. Proc. No. 619 (AIP, New York, 2001).
[19] H. Haberzettl *et al.*, Phys. Rev. C **58**, R40 (1998).
[20] Z. Liang and C. Boros, Phys. Rev. D **61**, 117503 (2000).